

Hierarchical Three-Body Problem at High Eccentricities = Simple Pendulum

II: Octupole including Brown’s Hamiltonian

Ygal Y. Klein^{Ⓛ*} and Boaz Katz^{Ⓛ†}

Dept. of Particle Phys. & Astrophys., Weizmann Institute of Science, Rehovot 76100, Israel

Accepted XXX. Received YYY; in original form ZZZ

ABSTRACT

The very long-term evolution of the hierarchical restricted three-body problem with a massive perturber is analyzed analytically in the high eccentricity regime. Perturbations on the time scale of the outer orbit can accumulate over long timescales and be comparable to the effect of the octupole term. These perturbations are described by Brown’s Hamiltonian - having different forms in the literature. We show that at the high eccentricity regime - the effect of Brown’s Hamiltonian is an azimuthal precession of the eccentricity vector and can be solved analytically. In fact, the dynamics are equivalent to a simple pendulum model allowing an explicit flip criterion.

Key words: gravitation-celestial mechanics-planets and satellites: dynamical evolution and stability-stars: multiple: close

1 INTRODUCTION

In this Letter we study analytically the long-term effect of a massive perturber in a three body system with a hierarchical configuration when the inner binary is at high eccentricity. Expanding the gravitational potential up to the leading order in the semi major axis ratio (quadrupole order) - Kozai (1962); Lidov (1962) analytically solved the oscillations of eccentricity and inclinations, since then called Kozai Lidov Cycles (KLCs)¹. The Eccentric Kozai Lidov (EKL) mechanism emerges when extending the expansion to the next order (octupole) which induces an asymmetry in the potential when the outer orbit is eccentric (Lithwick & Naoz 2011). The octupole term allows extremely high eccentricities associated with orbital flips - change of orientation of the orbit from prograde to retrograde (Katz et al. 2011; Naoz et al. 2011; Lithwick & Naoz 2011; Naoz et al. 2013) (for a review see Naoz (2016)). This effect was extensively studied numerically (Ford et al. 2000; Naoz et al. 2011; Lithwick & Naoz 2011; Naoz et al. 2013; Li et al. 2014; Lei 2022; Lei, Hanlun & Gong, Yan-Xiang 2022) and analytically (Katz et al. 2011; Sidorenko 2018; Lei, Hanlun & Gong, Yan-Xiang 2022; Weldon et al. 2024; Klein & Katz 2024). The EKL effect has been proposed to play a key role in a broad range of astrophysical phenomena including satellites, planets, and black hole mergers (Naoz et al. 2012; Teysandier et al. 2013; Petrovich 2015; Stephan et al. 2016; Liu & Lai 2018; Stephan et al. 2021; Angelo et al. 2022; Melchor et al. 2023).

The common approach to study the long term evolution of a hierarchical system is the double averaging (DA) approximation. For massive perturbers, where the ratio between the period of the outer orbit to the timescale of the KLCs is comparable to, or larger than,

the strength of the octupole term - the double averaging fails to reproduce the long term dynamics of the EKL (Luo et al. 2016; Will 2021; Tremaine 2023). The DA can be corrected by incorporating a correction to the Hamiltonian (Brown’s Hamiltonian (Brown 1936a,b,c; Soderhjelm 1975; Ćuk & Burns 2004; Breiter & Vokrouhlický 2015; Luo et al. 2016; Will 2021; Tremaine 2023)). Recently, Tremaine (2023) showed that the Hamiltonians provided in (Brown 1936c; Soderhjelm 1975; Breiter & Vokrouhlický 2015; Luo et al. 2016; Will 2021) are equivalent to each other up to small oscillating perturbations due to different choices of fictitious time (Will 2021). Moreover, Tremaine (2023) provided a new, significantly simplified, version of Brown’s Hamiltonian.

In a previous Paper (Klein & Katz (2024), hereafter referred to as Paper I), we have shown that in the high eccentricity regime, the EKL effect can be described using a simple pendulum model - with a flip criterion equivalent to the pendulum librating.

In this Letter, we extend the approach of Paper I using the new version of Brown’s Hamiltonian provided by Tremaine (2023) to analytically solve the effect of Brown’s Hamiltonian along with the octupole term. We show that using one of the forms of this Hamiltonian the combined effect can be described also by a simple pendulum with its velocity shifted by a constant, due to an additional azimuthal precession of the eccentricity vector.

2 COORDINATE SYSTEM

Consider a test particle orbiting a central mass m on an inner orbit with semimajor axis a and eccentricity e and a distant mass m_{per} on an outer orbit with $a_{\text{per}}, e_{\text{per}}$ where $a/a_{\text{per}} \ll 1$. Following Katz et al. (2011) we align the z axis along the direction of the total angular momentum vector (which is the angular momentum vector of the outer orbit since the inner orbit is of a test particle). The x axis is directed towards the pericenter of the (constant) outer orbit. The

* E-mail: ygalklein@gmail.com (YK)

† E-mail: boaz.katz@weizmann.ac.il (BK)

¹ See recent historical overview including earlier relevant work by von Zeipel (1910) in Ito & Ohtsuka (2019).

dynamics of the test particle can be parameterized by two dimensionless orthogonal vectors $\mathbf{j} = \mathbf{J}/\sqrt{GMa}$, where \mathbf{J} is the specific angular momentum vector, and \mathbf{e} a vector pointing in the direction of the pericenter with magnitude e . Using the variables i_e and Ω_e as in [Katz et al. \(2011\)](#) the eccentricity vector \mathbf{e} is given by

$$\mathbf{e} = e (\sin i_e \cos \Omega_e, \sin i_e \sin \Omega_e, \cos i_e). \quad (1)$$

Expanding the perturbing potential to the third order term in the small parameter a/a_{per} (the octupole term), averaging over the inner orbit, calculating the oscillations of \mathbf{j} and \mathbf{e} during an outer orbit and then averaging over the outer orbit results with the following potential:

$$\Phi_{\text{per}} = \Phi_0 \left(\phi_{\text{quad}} + \epsilon_{\text{oct}} \phi_{\text{oct}} + \epsilon_{\text{SA}} \phi_{\text{HB3}} \right) \quad (2)$$

where (e.g. [Katz et al. \(2011\)](#); [Liu et al. \(2014\)](#); [Petrovich \(2015\)](#); [Tremaine \(2023\)](#); [Luo et al. \(2016\)](#))

$$\phi_{\text{quad}} = \frac{3}{4} \left(\frac{1}{2} j_z^2 + e^2 - \frac{5}{2} e_z^2 - \frac{1}{6} \right), \quad (3)$$

$$\phi_{\text{oct}} = \frac{75}{64} \left(e_x \left(\frac{1}{5} - \frac{8}{5} e^2 + 7e_z^2 - j_z^2 \right) - 2e_z j_x j_z \right), \quad (4)$$

and (Equation 67 of [Tremaine \(2023\)](#))

$$\phi_{\text{HB3}} = -\frac{27}{64} \left(1 + \frac{2}{3} e_{\text{per}}^2 \right) j_z [(1 - j_z^2)/3 + 8e^2 - 5e_z^2], \quad (5)$$

$$\Phi_0 = \frac{Gm_{\text{per}}a^2}{a_{\text{per}}^3 \left(1 - e_{\text{per}}^2 \right)^{\frac{3}{2}}} \quad (6)$$

$$\epsilon_{\text{oct}} = \frac{a}{a_{\text{per}}} \frac{e_{\text{per}}}{1 - e_{\text{per}}^2} \quad (7)$$

$$\epsilon_{\text{SA}} = \left(\frac{a}{a_{\text{per}}} \right)^{3/2} \frac{1}{(1 - e_{\text{per}}^2)^{3/2}} \frac{m_{\text{per}}}{[(m + m_{\text{per}})m]^{1/2}} \quad (8)$$

with Φ_0 , ϵ_{oct} and ϵ_{SA} constant. Time and its derivatives are expressed in units of the secular timescale

$$t_{\text{sec}} = \sqrt{GMa}/\Phi_0 \quad (9)$$

using $\tau \equiv t/t_{\text{sec}}$ and obtaining $\epsilon_{\text{SA}} = \frac{P_{\text{out}}}{2\pi t_{\text{sec}}}$ measuring the ratio between the period of the outer orbit and the secular Kozai Lidov timescale.

3 SLOW VARIABLES

When $\epsilon_{\text{oct}} = 0$ (the periodic analytically solved KLCs) the perturbing potential is axisymmetric (with respect to the z axis) admitting a constant of the motion, j_z , which limits the eccentricity through the constraint $j > j_z$. When neglecting ϵ_{SA} KLCs are classified by the values of the constants j_z and

$$\begin{aligned} C_K &= \frac{4}{3} \phi_{\text{quad}} + \frac{1}{6} - \frac{1}{2} j_z^2 \\ &= e^2 - \frac{5}{2} e_z^2. \end{aligned} \quad (10)$$

When $C_K < 0$, the argument of pericenter of the inner orbit, ω , librates around $\frac{\pi}{2}$ or $-\frac{\pi}{2}$ (*librating* cycles), and when $C_K > 0$, it goes through all values $[0, 2\pi]$ (*rotating* cycles).

In the problem we study here with $\epsilon_{\text{oct}} > 0$ and without neglecting

ϵ_{SA} , C_K and j_z are no longer constant. The three slow variables j_z , C_K and Ω_e change slowly on a timescale of $\sim t_{\text{sec}}/\sqrt{\epsilon_{\text{oct}}}$ (see Eqs. 7-9) ([Antognini 2015](#)). As in [Katz et al. \(2011\)](#) we focus on the regime of high eccentricity, i.e. $|j_z| \ll 1$.

Up to leading order in j_z , we have from Equation 2 and Equation 20 of [Tremaine \(2023\)](#)

$$\dot{\Omega}_e = f_{\Omega} j_z - \epsilon_{\text{SA}} \left(1 + \frac{2}{3} e_{\text{per}}^2 \right) f_{\text{SA}} \quad (11)$$

$$\dot{j}_z = -\epsilon_{\text{oct}} f_j \sin \Omega_e$$

where

$$f_{\text{SA}} = \frac{27}{64} \left(\frac{1}{3} + 8C_K + 15e_z^2 \right) \quad (12)$$

$$\text{and } (Katz et al. 2011) f_j = (75/64) e \sin i_e \left(\frac{1}{5} - e^2 \left(\frac{8}{5} - 7 \cos^2 i_e \right) \right),$$

$$f_{\Omega} = 3 \left(4 - 3/\sin^2 i_e \right) / 4.$$

4 AVERAGED EQUATIONS

Averaging over rotating KLCs at $j_z = 0$ (up to the leading order in j_z and ϵ_{oct}) (librating KLCs with $|j_z| \ll 1$ accumulate change in j_z on a much longer timescale ([Katz et al. 2011](#))), the averaged equations for the long term evolution of Ω_e and j_z are

$$\dot{\Omega}_e = \langle f_{\Omega} \rangle j_z - \epsilon_{\text{SA}} \left(1 + \frac{2}{3} e_{\text{per}}^2 \right) \langle f_{\text{SA}} \rangle \quad (13)$$

$$\dot{j}_z = -\epsilon_{\text{oct}} \langle f_j \rangle \sin \Omega_e$$

where

$$\langle f_{\text{SA}} \rangle = \frac{27}{64} \left(\frac{1}{3} + 8C_K + 15 \langle e_z^2 \rangle \right), \quad (14)$$

$$\langle e_z^2 \rangle = \frac{2}{5} (1 - C_K) \frac{E(x) - (1-x)K(x)}{xK(x)}$$

and ([Katz et al. 2011](#))

$$\langle f_{\Omega} \rangle = \frac{6E(x) - 3K(x)}{4K(x)},$$

$$\langle f_j \rangle = \frac{15\pi}{128\sqrt{10}} \frac{1}{K(x)} (4 - 11C_K) \sqrt{6 + 4C_K}, \quad (15)$$

$$x = 3 \frac{1 - C_K}{3 + 2C_K}$$

and $K(m)$ and $E(m)$ are the complete elliptic functions of the first and second kind, respectively.

5 SIMPLE PENDULUM

As presented in [Paper I](#), since Φ_{per} is constant and $\epsilon_{\text{oct}} \phi_{\text{oct}}$, $\epsilon_{\text{SA}} \phi_{\text{HB3}}$ and j_z are small - C_K and therefore $\langle f_{\Omega} \rangle$, $\langle f_j \rangle$, $\langle f_{\text{SA}} \rangle$ are approximately constant, Equations 13 are equations of a simple pendulum with angle $\phi = \Omega_e$ where the product $\langle f_{\Omega} \rangle \langle f_j \rangle > 0$ and $\phi = \Omega_e + \pi$ otherwise. The velocity of the pendulum is given by

$$\dot{\phi} = \langle f_{\Omega} \rangle j_z - \Delta \quad (16)$$

with

$$\Delta = \epsilon_{\text{SA}} \left(1 + \frac{2}{3} e_{\text{per}}^2 \right) \langle f_{\text{SA}} \rangle \quad (17)$$

a positive constant. The pendulum has a constant energy

$$E = \frac{1}{2} \left(\dot{\phi}^0 \right)^2 + V^0 \quad (18)$$

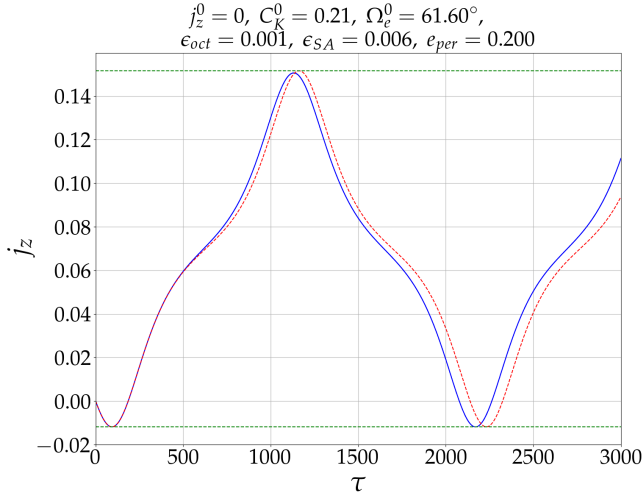


Figure 1. Results of a numeric integration of the double averaged equations (blue) along with the result of a simple pendulum (Equations 13, red). The values of the initial conditions and ϵ_{oct} , ϵ_{SA} and e_{per} are shown above the plot. Shown is j_z as a function of (normalized) time. The two green horizontal lines are the maximum and minimum values of j_z of the simple pendulum.

where the potential V is given by

$$V = \epsilon_{\text{oct}} |\langle f_{\Omega} \rangle \langle f_j \rangle| (1 - \cos \phi). \quad (19)$$

An example of a numerical integration of the full double averaged equations (Equations 20 in Tremaine (2023)) compared with the solution of Equations 13 with the approximation of constants $\langle f_{\Omega} \rangle$, $\langle f_j \rangle$, $\langle f_{\text{SA}} \rangle$ (evaluated at C_K^0) is shown in Figure 1. As can be seen - for the example shown - the long term evolution of j_z is successfully approximated by equations of a simple pendulum.

5.1 Scaling

The potential for Brown Hamiltonian in its HB3 form, Equation 5, is axis symmetric (with respect to the z -axis). Denoting the longitude of ascending node as Ω leads, at low j_z , to $\dot{\Omega} = \dot{\Omega}_e$ being independent of Ω_e making the effective equations for the slow variables to be equations of a simple pendulum with the velocity shifted by a constant (Δ , Equation 17). As presented in Paper I, the velocity in the pendulum model, i.e. j_z there - scales as $\sqrt{\epsilon_{\text{oct}}}$. Therefore, adding the constant Δ to the effective equations to account for Brown's Hamiltonian - makes the equations scale with a scaling factor of

$$s = \frac{\epsilon_{\text{SA}} \left(1 + \frac{2}{3} e_{\text{per}}^2\right)}{\sqrt{\epsilon_{\text{oct}}}}. \quad (20)$$

6 FLIPS

A flip - zero crossing of j_z - happens when the product $j_z^{\text{max}} j_z^{\text{min}} < 0$. Using Equation 16 we have for example where $\langle f_{\Omega} \rangle > 0$, i.e. for $C_K^0 \gtrsim 0.112$

$$j_z^{\text{max}} = \frac{1}{\langle f_{\Omega} \rangle} (\phi^{\text{max}} + \Delta) \quad (21)$$

and similar expression for j_z^{min} (and vice-versa when $\langle f_{\Omega} \rangle < 0$ at $C_K^0 \lesssim 0.112$). Since the analytic model is a simple pendulum model, obtaining ϕ^{max} and ϕ^{min} is straightforward. Given ϵ_{oct} , ϵ_{SA} and e_{per}

and initial values j_z^0 , C_K^0 and Ω_e^0 , the simple pendulum can be in either mode, *Libration* when $E < 2\epsilon_{\text{oct}} |\langle f_j \rangle \langle f_{\Omega} \rangle|$ or otherwise in *Rotation*.

6.1 Maximal Deviation of j_z from $j_z^0 = 0$

Within the approximation of constant C_K , one way of obtaining the value of maximal j_z^0 allowing a flip is evaluating the maximal deviation of j_z from $j_z^0 = 0$. For example, starting with $j_z^0 = 0$ we have for the maximal available value of j_z^{max} : Given ϵ_{oct} , ϵ_{SA} and e_{per} and C_K^0 the condition for a possibility of libration of the pendulum is

$$\frac{\Delta^2}{2\epsilon_{\text{oct}} |\langle f_j \rangle \langle f_{\Omega} \rangle|} \leq 2. \quad (22)$$

If $\langle f_{\Omega} \rangle > 0$ (i.e. $C_K^0 \gtrsim 0.112$) and libration is possible (Equation 22) the envelopes of the different regimes are given by

$$0 \leq j_z^{\text{max, rotation}} \leq \frac{\Delta}{\langle f_{\Omega} \rangle} \quad (23)$$

$$2 \frac{\Delta}{\langle f_{\Omega} \rangle} \leq j_z^{\text{max, libration}} \leq \frac{\Delta}{\langle f_{\Omega} \rangle} + 2 \sqrt{\epsilon_{\text{oct}} \left| \frac{\langle f_j \rangle}{\langle f_{\Omega} \rangle} \right|}.$$

If libration is not possible, the envelope is given by

$$0 \leq j_z^{\text{max, rotation}} \leq \frac{\Delta - \sqrt{\Delta^2 - 4\epsilon_{\text{oct}} |\langle f_j \rangle \langle f_{\Omega} \rangle|}}{\langle f_{\Omega} \rangle}. \quad (24)$$

If $\langle f_{\Omega} \rangle < 0$ (i.e. $C_K^0 \lesssim 0.112$) and libration is possible the envelopes of the different regimes are given by

$$\frac{\Delta}{\langle f_{\Omega} \rangle} + 2 \sqrt{\epsilon_{\text{oct}} \left| \frac{\langle f_j \rangle}{\langle f_{\Omega} \rangle} \right|} \leq j_z^{\text{max, rotation}} \leq \frac{\Delta - \sqrt{\Delta^2 + 4\epsilon_{\text{oct}} |\langle f_j \rangle \langle f_{\Omega} \rangle|}}{\langle f_{\Omega} \rangle}.$$

$$0 \leq j_z^{\text{max, libration}} \leq \frac{\Delta}{\langle f_{\Omega} \rangle} + 2 \sqrt{\epsilon_{\text{oct}} \left| \frac{\langle f_j \rangle}{\langle f_{\Omega} \rangle} \right|}. \quad (25)$$

If libration is not possible, the envelope is given by

$$0 \leq j_z^{\text{max, rotation}} \leq \frac{\Delta - \sqrt{\Delta^2 + 4\epsilon_{\text{oct}} |\langle f_j \rangle \langle f_{\Omega} \rangle|}}{\langle f_{\Omega} \rangle}. \quad (26)$$

Similar expressions can be obtained for j_z^{min} . The maximal and minimal values of j_z obtained in 1000 numerical simulations with $j_z^0 = e_z^0 = 0$ (i.e. $i^0 = 0$, $\omega^0 = 0$) and randomly chosen initial conditions (uniformly distributed in j_x and e_y) are plotted using black crosses in Figure 2 for $\epsilon_{\text{oct}} = 0.001$, $\epsilon_{\text{SA}} = 0.006$ and $e_{\text{per}} = 0.2$. The black line in Figure 2 comes from Equation 12 of Paper I and is the envelope of both j_z^{max} and j_z^{min} in the analytic model when Brown's Hamiltonian is not taken into account (i.e. $\epsilon_{\text{SA}} = 0$). The red regions denote allowed results from librating pendulums while blue regions denote rotating pendulums (through Equations 22-26). As can be seen, the shaded regions agree with the envelope of the numerically available j_z^{max} and j_z^{min} and predict the splitting of allowed regions between librating and rotating pendulums. The analytic model allows for a prediction of the maximal deviation for each set of initial conditions and these are shown in a similar plot in appendix B.

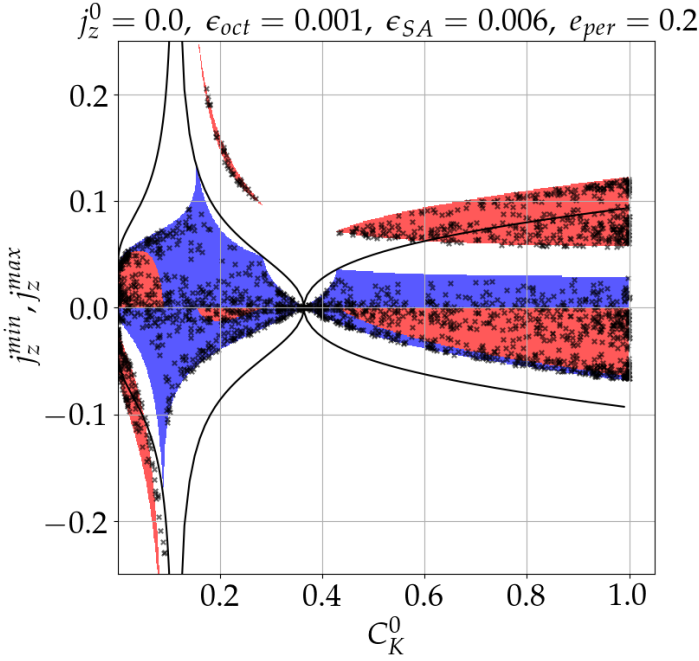


Figure 2. j_z^{\max} and j_z^{\min} vs. C_K^0 when $j_z^0 = e_z^0 = 0$ and all other components randomly chosen (uniformly distributed in j_x and e_y) for 1000 realizations of initial conditions. The results of direct numerical integrations of the double averaged equations (up to $\tau = 10/\epsilon_{\text{oct}}$) are shown using black crosses. The envelope of the analytic model of the simple pendulum from Paper I is shown using a black curve (depends only on ϵ_{oct}). Blue regions denote the analytic prediction for rotating pendulums and red regions denote the analytic prediction for librating pendulums through Equations 22-26.

6.1.1 Dependence on ϵ_{oct} , ϵ_{SA} and e_{per}

Using the scaling factor defined in section 5.1 an evaluation of the maximal available deviation of j_z from $j_z^0 = 0$ can be presented. For each C_K^0 (and $j_z^0 = 0$) there is a special value of s separating the parameter space of ϵ_{oct} , ϵ_{SA} and e_{per} between pendulums that can librate (for some Ω_0^0) and pendulums that can only rotate:

$$s^{\text{libration possible}} < \frac{128}{27} \frac{\sqrt{|\langle f_j \rangle \langle f_\Omega \rangle|}}{\left(\frac{1}{3} + 8C_K + 15 \langle e_z^2 \rangle\right)}. \quad (27)$$

Given the parameters ϵ_{oct} , ϵ_{SA} and e_{per} and initial values C_K^0 and $\omega^0 = 0$ and $j_z^0 = 0$ the maximal attainable value of j_z^{\max} can be evaluated both numerically (by scanning all possible values of Ω^0) and analytically using the simple pendulum model (through ϕ^{\max} and ϕ^{\min}). These evaluations are plotted in Figure 3 showing the agreement between different values of the parameters when scaled using s . Each subplot presents results for some value of C_K^0 (written above the subplot). We scan 4 values of $\epsilon_{\text{oct}} = 0.0001$ (blue), 0.001 (cyan), 0.01 (magenta) and 0.1 (black). For ϵ_{SA} we scan 19 values logarithmically spaced between 0.0001 and 0.1 and for e_{per} we use the values 0.05, 0.2, 0.5, 0.7 and 0.9. Each cross represents the maximal value of j_z^{\max} obtained from 36 simulations with Ω_0 equally spaced by 10° between 0 and 360° . The red curve denotes the prediction of the simple pendulum model using Equations 22-26. Note that the deviation of the black crosses (denoting simulations with $\epsilon_{\text{oct}} = 0.1$) from a simple pendulum model is present already in in Figure 4 of Paper I presenting the results of a simple pendulum model for the "no Brown's Hamiltonian" equations (i.e when $\epsilon_{\text{SA}} = 0$). As s

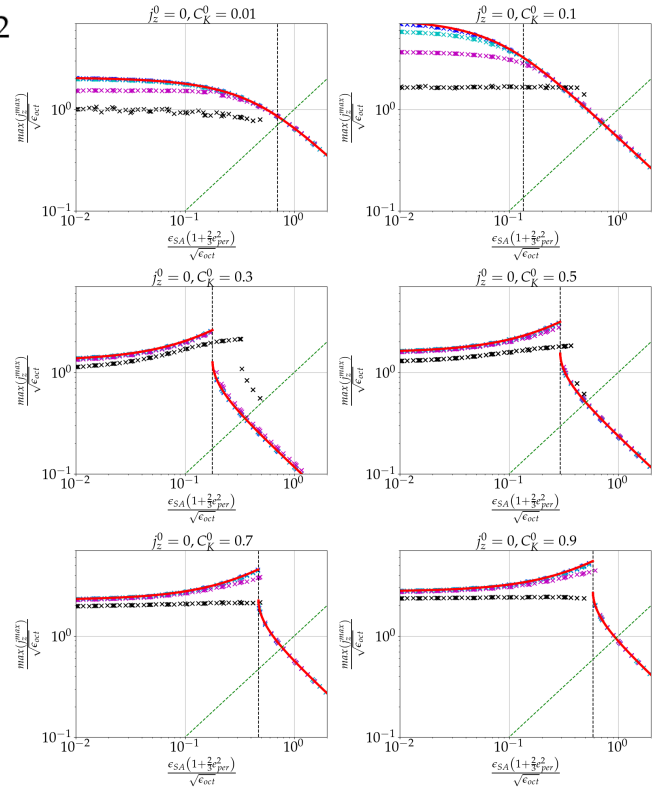


Figure 3. The maximal attainable value of $\frac{j_z^{\max}}{\sqrt{\epsilon_{\text{oct}}}}$ from $j_z^0 = e_z^0 = 0$ vs. the scaling factor s (Equation 20). Each panel has a **different** value of the initial C_K shown above the plot. The vertical black dashed curve denotes the value of $s^{\text{libration possible}}$ (Equation 27). Each cross is a result of 36 numerical integrations with the same ϵ_{oct} , ϵ_{SA} , e_{per} , $\omega^0 = 0$, $j_z^0 = 0$, C_K^0 and denote the maximal value of j_z^{\max} over a scan of all possible values of Ω^0 (equally spaced by 10° between 0 and 360°). Shown are four values of $\epsilon_{\text{oct}} = 0.0001$ (blue), 0.001 (cyan), 0.01 (magenta) and 0.1 (black). The values of ϵ_{SA} are scanned using a logarithmic spacing of 19 values between 0.0001 and 0.1. The values of e_{per} are taken from the set 0.05, 0.2, 0.5, 0.7 and 0.9. The red curve denotes the prediction of the simple pendulum model using Equations 22-26. The green dashed line is a line of $y = x$ schematically presenting the scale of the fluctuations effect from Haim & Katz (2018).

increases, i.e as ϵ_{SA} increases, a different mechanism, fluctuations in j_z during close approaches (Haim & Katz 2018), becomes dominant as its effect scales as $j_z^{\max} \sim \epsilon_{\text{SA}}$ (see Equation 13 of Haim & Katz (2018)). A scale of this effect is schematically plotted in Figure 3 using a dashed green line. All in all, the inclusion of just Brown's Hamiltonian is important in the portion of phase space of s shown in Figure 3 for not too low values (where the octupole term is much stronger than Brown's Hamiltonian) and not too high values where other mechanisms must be taken into account as well. As presented in Equations 22-26 and in Figure 2 there is a difference between the region where $\langle f_\Omega \rangle > 0$ ($C_K^0 \gtrsim 0.112$) where the maximal value of j_z^{\max} is obtained in librating region if they are possible to the region where $\langle f_\Omega \rangle < 0$ ($C_K^0 \lesssim 0.112$) where the the maximal value of j_z^{\max} is obtained from rotating pendulums even when libration is possible. This is the origin of the sharp peaks seen in the panels of Figure 3 with C_K^0 values greater than ≈ 0.112 and are absent for the two upper panels with $C_K^0 = 0.01, 0.1$ with $\langle f_\Omega \rangle < 0$.

6.2 flip criterion

Another form of a flip criterion is a map from initial conditions to a flip or non flip outcome. Given ϵ_{oct} , ϵ_{SA} and e_{per} and initial values f_z^0 , C_K^0 and Ω^0 (with $\omega^0 = 0$), a condition for whether a flip would occur can be obtained using the simple pendulum model. When the pendulum is in libration for example, a flip will occur if

$$\frac{1}{2}\Delta^2 < E < 2\epsilon_{\text{oct}} |\langle f_j \rangle \langle f_\Omega \rangle| \quad (28)$$

where the right hand side is the libration condition and the left hand side is the flip criterion when in libration. When the pendulum is in rotation mode the flip criterion is more complex and is given in appendix A. A comparison between a numerical *flip map* and the analytic prediction of the simple pendulum model (Equations A3, A5) as a function of i^0 and Ω^0 is shown in Figure 4 for $\epsilon_{\text{oct}} = 0.001$, $\epsilon_{\text{SA}} = 0.006$ and $e_{\text{per}} = 0.2$. Each point represent the result of a numerical simulation of the double averaged equations (up to $\tau = 10/\epsilon_{\text{oct}}$) with $\omega^0 = 0$, and $C_K^0 = (e^0)^2$ written above each subplot. A point is marked red if a flip occurred and blue otherwise. Black curves mark the analytic prediction of the flip criterion using the simple pendulum model via Equations A3, A5. As can be seen, the black curve follows the border between red and blue points for the wide range of C_K^0 values resulting with different forms of a flip map.

7 DISCUSSION

In this study, we extended the approach presented in Paper I to analytically solve the EKL effect at high eccentricities, incorporating Brown’s Hamiltonian. Using the simplified version of Brown’s Hamiltonian from Tremaine (2023), we demonstrated that its prominent effect on long-term evolution is an additional precession of the eccentricity vector. The dynamics can be described using a simple pendulum model where the additional term imposes a shift in the the pendulum’s velocity. This model allows for the derivation of an explicit flip criterion (Figure 4) dependent on whether the equivalent simple pendulum being in rotation or libration (Equations A3, A5).

The effective equations obtained introduce a scaling factor, s (Equation 20), which measures the importance of including Brown’s Hamiltonian relative to the octupole term (Figure 3). When the $s \lesssim 0.1$ - the dynamics are dominated by the octupole term alone. For $s \gtrsim 1$ additional effects need to be considered (e.g. Luo et al. (2016); Haim & Katz (2018)). This identifies the region of $0.1 \lesssim s \lesssim 1$ where the inclusion of (just) Brown’s Hamiltonian is crucial for accurately the high eccentricity dynamics and obtaining a physical understanding of the flip criterion through the analytical model.

For example, consider the parameters used in this Letter: $\epsilon_{\text{oct}} = 0.001$ and $\epsilon_{\text{SA}} = 0.006$ (with $e_{\text{per}} = 0.2$) leading to a scaling factor $s \approx 0.2$. These values correspond to a hierarchical system with $m_{\text{per}}/m \sim 300$ and $a_{\text{per}}/a \sim 200$. Consider a Jupiter-sized planet orbiting an M-dwarf of mass $m_{\text{per}} = 0.3M_\odot$ on an orbit with $a_{\text{per}} = 5\text{AU}$. A satellite orbiting the Jupiter at $a \sim 0.025\text{AU}$ has a scaling factor $s \approx 0.2$, indicating that including (just) Brown’s Hamiltonian in addition to the octupole term is necessary for accurately describing its dynamics. In the high eccentricity regime, this system can be analytically investigated using the simple pendulum model.

DATA AVAILABILITY

The codes used in this article will be shared on reasonable request.

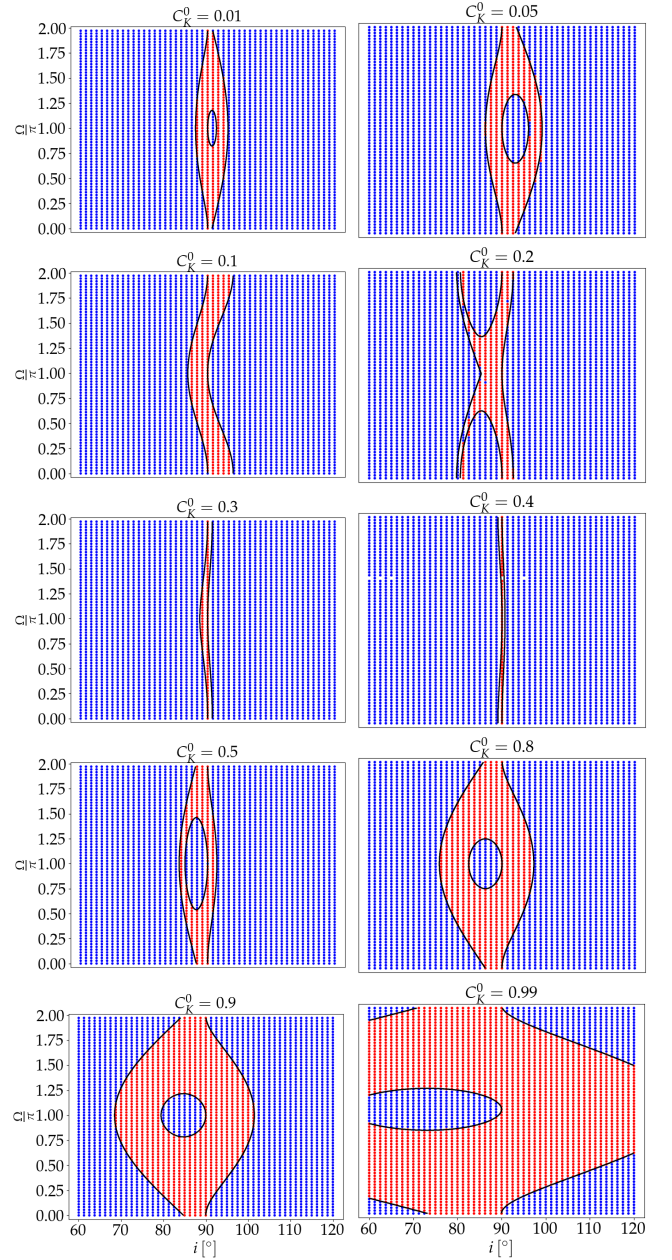


Figure 4. Parameter space of orbital flips from the solution of the double averaged secular equations (up to $\tau = 10/\epsilon_{\text{oct}}$). All panels have the same values of $\epsilon_{\text{oct}} = 0.001$, $\epsilon_{\text{SA}} = 0.006$ and $e_{\text{per}} = 0.2$. Each panel have a **different** value of the initial C_K shown above the plot. All integrations have $\omega^0 = 0$ and the initial values of inclination and Ω are scanned. Red points denote integrations where a flip occurred and blue points denote these without a flip. Black curves denote the flip criterion of the simple pendulum model (Equations A3- A5 and the separation between librating and rotating pendulum).

REFERENCES

- Angelo I., Naoz S., Petigura E., MacDougall M., Stephan A. P., Isaacson H., Howard A. W., 2022, *The Astronomical Journal*, 163, 227
 Antognini J. M. O., 2015, *Monthly Notices of the Royal Astronomical Society*, 452, 3610
 Breiter S., Vokrouhlický D., 2015, *Monthly Notices of the Royal Astronomical Society*, 449, 1691
 Brown E. W., 1936a, *Monthly Notices of the Royal Astronomical Society*,

- 97, 56
- Brown E. W., 1936b, *Monthly Notices of the Royal Astronomical Society*, 97, 62
- Brown E. W., 1936c, *Monthly Notices of the Royal Astronomical Society*, 97, 116
- Ford E. B., Kozinsky B., Rasio F. A., 2000, *The Astrophysical Journal*, 535, 385
- Haim N., Katz B., 2018, *Monthly Notices of the Royal Astronomical Society*, 479, 3155
- Ito T., Ohtsuka K., 2019, *Monographs on Environment, Earth and Planets*, 7, 1
- Katz B., Dong S., Malhotra R., 2011, *Phys. Rev. Lett.*, 107, 181101
- Klein Y. Y., Katz B., 2024, *arXiv e-prints*, p. arXiv:2407.07154
- Kozai Y., 1962, *The Astronomical Journal*, 67, 591
- Lei H., 2022, *The Astronomical Journal*, 163, 214
- Lei, Hanlun Gong, Yan-Xiang 2022, *A&A*, 665, A62
- Li G., Naoz S., Kocsis B., Loeb A., 2014, *The Astrophysical Journal*, 785, 116
- Lidov M., 1962, *Planetary and Space Science*, 9, 719
- Lithwick Y., Naoz S., 2011, *The Astrophysical Journal*, 742, 94
- Liu B., Lai D., 2018, *The Astrophysical Journal*, 863, 68
- Liu B., Muñoz D. J., Lai D., 2014, *Monthly Notices of the Royal Astronomical Society*, 447, 747
- Luo L., Katz B., Dong S., 2016, *Monthly Notices of the Royal Astronomical Society*, 458, 3060
- Melchor D., Mockler B., Naoz S., Rose S. C., Ramirez-Ruiz E., 2023, *The Astrophysical Journal*, 960, 39
- Naoz S., 2016, *Annual Review of Astronomy and Astrophysics*, 54, 441
- Naoz S., Farr W. M., Lithwick Y., Rasio F. A., Teyssandier J., 2011, *Nature*, 473, 187
- Naoz S., Farr W. M., Rasio F. A., 2012, *The Astrophysical Journal Letters*, 754, L36
- Naoz S., Farr W. M., Lithwick Y., Rasio F. A., Teyssandier J., 2013, *Monthly Notices of the Royal Astronomical Society*, 431, 2155
- Petrovich C., 2015, *The Astrophysical Journal*, 799, 27
- Sidorenko V. V., 2018, *Celestial Mechanics and Dynamical Astronomy*, 130, 4
- Soderhjelm S., 1975, *A&A*, 42, 229
- Stephan A. P., Naoz S., Ghez A. M., Witzel G., Sitarski B. N., Do T., Kocsis B., 2016, *Monthly Notices of the Royal Astronomical Society*, 460, 3494
- Stephan A. P., Naoz S., Gaudi B. S., 2021, *ApJ*, 922, 4
- Teyssandier J., Naoz S., Lizarraga I., Rasio F. A., 2013, *The Astrophysical Journal*, 779, 166
- Tremaine S., 2023, *Monthly Notices of the Royal Astronomical Society*, 522, 937
- Weldon G. C., Naoz S., Hansen B. M. S., 2024, Analytical models for secular descents in hierarchical triple systems ([arXiv:2405.20377](https://arxiv.org/abs/2405.20377))
- Will C. M., 2021, *Phys. Rev. D*, 103, 063003
- von Zeipel H., 1910, *Astronomische Nachrichten*, 183, 345
- Čuk M., Burns J. A., 2004, *The Astronomical Journal*, 128, 2518

APPENDIX A: EXPLICIT FLIP CRITERION

A flip - zero crossing of j_z - happens when the product $j_z^{\max} j_z^{\min} < 0$. From Equation 16 we obtain expressions for j_z^{\max} and j_z^{\min} : For $C_K^0 \gtrsim 0.112$ where $\langle f_\Omega \rangle > 0$

$$j_z^{\max} = \frac{1}{\langle f_\Omega \rangle} (\phi^{\max} + \Delta) \quad (A1)$$

$$j_z^{\min} = \frac{1}{\langle f_\Omega \rangle} (\phi^{\min} + \Delta)$$

and vice-versa where $\langle f_\Omega \rangle < 0$. The condition for a flip depends on the initial conditions and specifically differs between two separate states of the pendulum: (i) Libration: When $E < 2 |\epsilon_{\text{oct}} \langle f_j \rangle \langle f_\Omega \rangle|$ the

pendulum is in libration mode, i.e $\phi^{\max} = \sqrt{2E}$ and $\phi^{\min} = -\sqrt{2E}$. In this case, j_z^{\max} and j_z^{\min} have different signs if

$$\Delta < \sqrt{2E} \quad (A2)$$

and this is the flip criterion if the pendulum is in libration. Given ϵ_{oct} , ϵ_{SA} and e_{per} and initial values j_z^0 , C_K^0 and Ω_e^0 if both inequalities are obeyed

$$\left(\langle f_\Omega \rangle j_z^0 \right)^2 - 2 \langle f_\Omega \rangle \Delta j_z^0 + 2 |\epsilon_{\text{oct}} \langle f_j \rangle \langle f_\Omega \rangle| (1 - \cos \phi^0) > 0$$

$$\frac{1}{2} \left(\langle f_\Omega \rangle j_z^0 - \Delta \right)^2 - |\epsilon_{\text{oct}} \langle f_j \rangle \langle f_\Omega \rangle| (1 + \cos \phi^0) < 0 \quad (A3)$$

a flip occurs. (ii) Rotation: When $E > 2 |\epsilon_{\text{oct}} \langle f_j \rangle \langle f_\Omega \rangle|$ the pendulum is in rotation mode, and ϕ does not change its sign. Since $\Delta > 0$ there is no flip if $\phi^0 > 0$. If $\phi^0 < 0$, $\phi^{\max} = -\sqrt{2(E - 2 |\epsilon_{\text{oct}} \langle f_j \rangle \langle f_\Omega \rangle|)}$ and $\phi^{\min} = -\sqrt{2E}$. A flip occurs if

$$|\phi^{\max}| < |\phi^{\min}| \quad (A4)$$

i.e if the following inequalities are obeyed

$$\left(\langle f_\Omega \rangle j_z^0 \right)^2 - 2\Delta \langle f_\Omega \rangle j_z^0 + 2 |\epsilon_{\text{oct}} \langle f_j \rangle \langle f_\Omega \rangle| (1 - \cos \phi^0) > 0$$

$$\left(\langle f_\Omega \rangle j_z^0 \right)^2 - 2\Delta \langle f_\Omega \rangle j_z^0 - 2 |\epsilon_{\text{oct}} \langle f_j \rangle \langle f_\Omega \rangle| (1 + \cos \phi^0) < 0$$

$$\frac{1}{2} \left(\langle f_\Omega \rangle j_z^0 - \Delta \right)^2 - |\epsilon_{\text{oct}} \langle f_j \rangle \langle f_\Omega \rangle| (1 + \cos \phi^0) > 0$$

$$\langle f_\Omega \rangle j_z^0 - \Delta < 0 \quad (A5)$$

The third inequality is the rotation condition. The fourth inequality is the negative ϕ^0 condition and the first two inequalities are the flip criterion for the rotation region.

APPENDIX B: J_Z^{MAX} AND J_Z^{MIN} FROM $J_Z^0 = E_Z^0 = 0$

In Figure B1 we plot the same information as Figure 2 but we add the prediction of the simple pendulum model for each set of random initial conditions using magenta open circles. As can be seen there, the predictions of Equations 21 for different values of Ω_e^0 agree with the numerical results to an excellent approximation.

This paper has been typeset from a \LaTeX file prepared by the author.

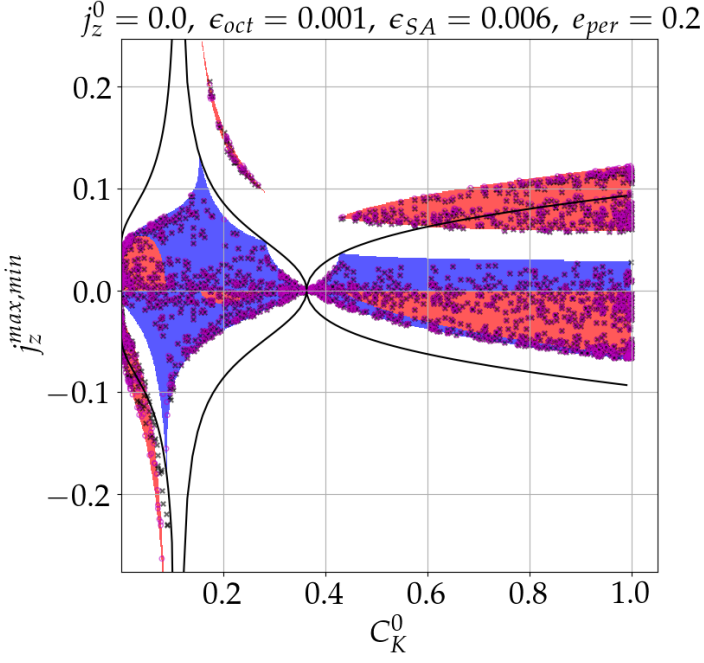


Figure B1. j_z^{\max} and j_z^{\min} vs. C_K^0 when $j_z^0 = e_z^0 = 0$ and all other components randomly chosen (uniformly distributed in j_x and e_y). The results of direct numerical integrations of the double averaged equations (up to $\tau = 10/\epsilon_{oct}$) are shown using black crosses. The envelope of the analytic model of the simple pendulum from [Paper I](#) is shown using a black curve (depends only on ϵ_{oct}). Blue regions denote the analytic prediction for rotating pendulums and red regions denote the analytic prediction for librating pendulums. Magenta open circles denote the prediction of the simple pendulum model for each set of initial conditions.